

Characteristics of the rotor R4-31 for the O4 NCal system VIR-0895B-22

Eddy Dangelser, Dimitri Estevez, Benoit Mours,
Mehmet Ozturk, Antoine Syx

IPHC-Strasbourg

September 19, 2022

Contents

| | | |
|----------|--|-----------|
| 1 | Introduction | 2 |
| 2 | Measurement method | 2 |
| 2.1 | Thermal effects and density | 3 |
| 3 | Raw measurements of the rotor | 4 |
| 4 | Extracting the geometrical parameters | 4 |
| 4.1 | Thickness | 4 |
| 4.2 | Radius | 5 |
| 5 | Characterization of the rotor using a simple model | 6 |
| 5.1 | Thickness | 7 |
| 5.2 | Radius | 7 |
| 5.3 | Analytical model of the rotor | 7 |
| 5.4 | Effects of the mirror geometry on the 3f signal | 8 |
| 5.5 | Signal uncertainties for the simple model | 8 |
| 6 | Characterization of the rotor using an advanced model | 9 |
| 6.1 | Thickness | 9 |
| 6.2 | Radius | 9 |
| 6.3 | Counterweight | 9 |
| 6.4 | Opening angles and asymmetry | 10 |
| 6.4.1 | Measurements | 10 |
| 6.4.2 | Uncertainty | 10 |
| 6.5 | Expected NCal signals and uncertainties | 11 |
| 6.5.1 | Advanced geometry including chamfers and counterweight | 11 |
| 6.5.2 | Remaining geometry uncertainty | 12 |
| 6.5.3 | Uncertainties | 13 |
| A | Appendix | 14 |

This note is a revised version of the previous release, a typo was corrected in eq. (11) where the term d^5 was previously mistyped as d^3 .

1 Introduction

This note follows the same discussion made on the rotor R4-01 in [VIR-0591C-22](#) and R4-05 in [VIR-0859A-22](#). This rotor has three sectors (see fig. 1 and the drawing at the end of this note) to produce a signal at 3f in the interferometer, the theoretical dimensions of the sectors are the same as the other rotors excepts for the opening angle which is $\alpha = \pi/3$.

The rotor has been engraved IPHC-R4-R4 on one side and sandblasted on the two other sides.

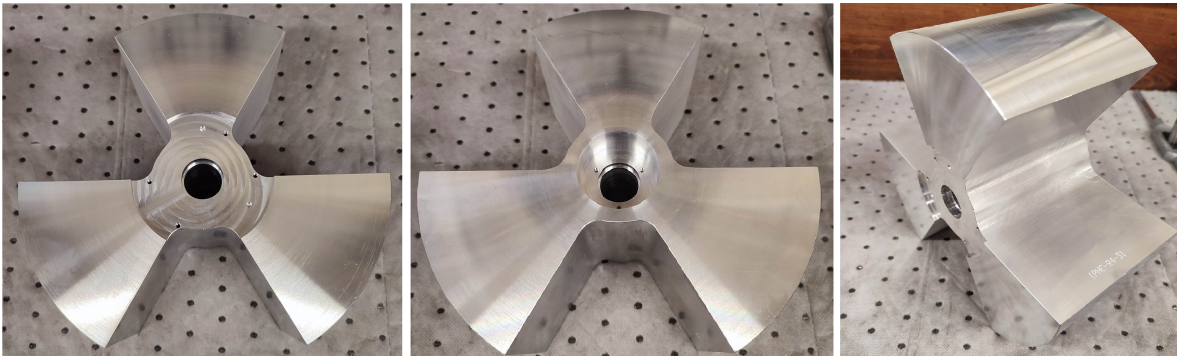


Figure 1: Pictures of the rotor. From left to right, the up face, the down face and a side view with the engraving.

2 Measurement method

To determine the geometry of the rotor we will use the same method as for R4-01 (see [VIR-0591C-22](#)) but considering three sectors. The thickness was measured using $24 \times 3 = 72$ points (see fig. 2) and the outer diameter was measured using $4 \times 3 = 12$ points.

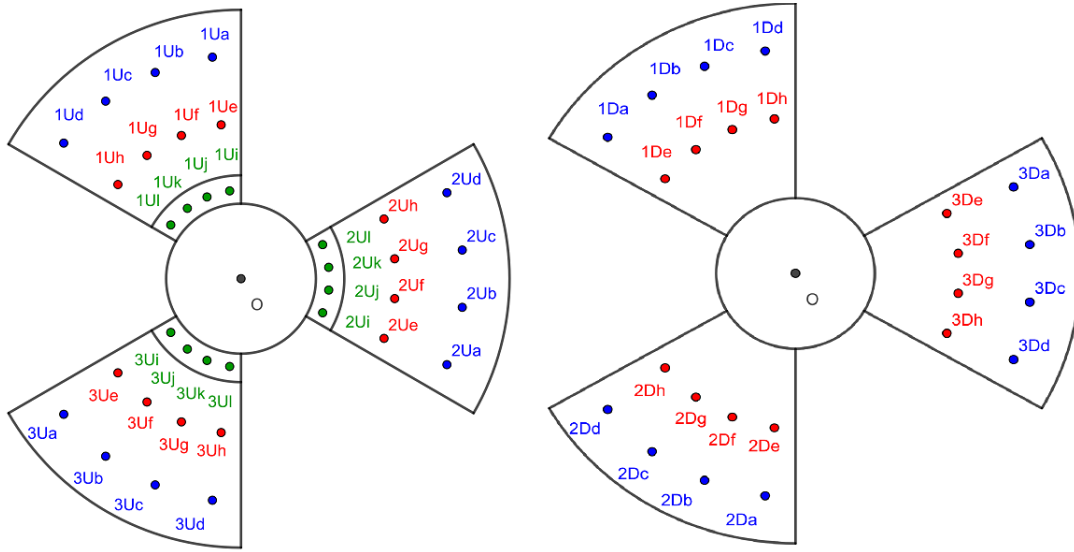


Figure 2: Outline of the faces of the rotor with the measurement points. Left figure is face up, right figure is face down. Sectors have been labelled 1,2 and 3.

The tool used to measure the thickness and the outer diameter is a measuring column "Garant 44 5350_600 HC1" (see [VIR-0160A-22](#)) with a given precision of $1.8+L/600 \mu\text{m}$ (L the measured length in mm).

The measuring column was operated on a metrology table with a value range from 0 to 2 μm . The rms of the 16 values is 0.9 μm .

We measured the opening angles of the sectors using a video measuring microscope "Garant MM2" (see [VIR-0591C-22](#)) with a given precision of $2.9+L/100 \mu\text{m}$ at 95% CL (L the measured length in mm).

2.1 Thermal effects and density

The rotor R4-31 has been machined from the same aluminum block as R4-05 described in [VIR-0859A-22](#). As for R4-05 the results will be expressed at a reference temperature of 23°C.

The density of the rotor R4-31 is $2810.8 \pm 0.2 \text{ kg.m}^{-3}$. This density is measured in air, if the rotor is used under vacuum, the density should be increased by the air density ($\rho_{air}=1.3 \text{ kg.m}^{-3}$).

The uncertainty on the strain h at 3f is the following (see eq. (12) for complete formula of the strain):

$$\begin{aligned} h &\propto \rho_{rot} b r_{max}^5 \\ &\propto \frac{m r_{max}^3}{\pi} \end{aligned} \quad (1)$$

Using $r(T) = r(1 + \alpha_T)$ (with the temperature factor $\alpha_T = C_T(T - T_{ref})$) we have:

$$\begin{aligned} h(T) &\propto r_{max}^3(T) \\ &\propto r_{max}^3(1 + \alpha_T)^3 \end{aligned} \quad (2)$$

We compute the relative uncertainty of h on the temperature T :

$$\left| \frac{\partial h}{\partial T} \right| \frac{\Delta T}{h} = \frac{3C_T}{1 + C_T(T - T_{ref})} \Delta T \quad (3)$$

This formula will be later used to compute the effect of the temperature on the signal strain.

3 Raw measurements of the rotor

This section presents the raw measurements made on the rotor at the ambient temperature of 23.1°C for the thickness and 26.9°C for the radius. Table 1 shows the thickness measurements according to the measurement points defined in figure 2. The rotor is laying on the table. The rotor surface as well as the table are not perfectly flat. Some space could be present in between that should be subtracted when computing the rotor thickness as discussed later.

| Measurement point | Sector 1 | | Sector 2 | | Sector 3 | |
|-------------------|----------|---------|----------|---------|----------|---------|
| | Up | Down | Up | Down | Up | Down |
| a | 104.467 | 104.468 | 104.396 | 104.400 | 104.406 | 104.406 |
| b | 104.468 | 104.470 | 104.406 | 104.408 | 104.399 | 104.400 |
| c | 104.466 | 104.469 | 104.417 | 104.418 | 104.391 | 104.390 |
| d | 104.459 | 104.464 | 104.429 | 104.428 | 104.383 | 104.380 |
| e | 104.469 | 104.468 | 104.422 | 104.429 | 104.427 | 104.428 |
| f | 104.469 | 104.469 | 104.428 | 104.432 | 104.422 | 104.422 |
| g | 104.468 | 104.468 | 104.438 | 104.439 | 104.416 | 104.416 |
| h | 104.464 | 104.465 | 104.446 | 104.446 | 104.416 | 104.412 |
| i | 101.652 | | 101.648 | | 101.649 | |
| j | 101.651 | | 101.647 | | 101.649 | |
| k | 101.653 | | 101.648 | | 101.649 | |
| l | 101.653 | | 101.648 | | 101.648 | |

Table 1: Raw measurements of the height in mm for each point at 23.1°C on L and R sectors of R4-31.

Table 2 displays the radius measurements. For this set of measurements, the axis was mounted on the rotor and the column was used to directly measure the radius of each sector by subtracting the diameter of the axis. The measurements were made on 4*3 diameters (four measurements per sector).

| Measurement point | Sector 1 | Sector 2 | Sector 3 |
|-------------------|----------|----------|----------|
| 1 | 103.943 | 103.998 | 104.012 |
| 2 | 103.960 | 104.003 | 104.030 |
| 3 | 103.973 | 103.991 | 104.035 |
| 4 | 103.958 | 103.966 | 104.020 |

Table 2: Raw measurements of the radius in mm for each point at 26.9°C on R4-31.

Theoretical values were taken for the inner radius $r_{\min} = 29$ mm and the up face radius for the counterweight $r_{\text{counterweight}} = 40$ mm (see drawing attached at the end of this note for values).

4 Extracting the geometrical parameters

4.1 Thickness

We need to correct the possible gap between the rotor and the measuring table. Assuming that the table is flatter than the rotor surface we can extract the gap from the measurement of the top surface considering the plane tangents to the highest points (asking them to be on both sectors). For this rotor these points are 1Uf,

2Uh, 3Ue for the up and 1Db, 2Dh, 3De for the down face (see fig. 2). Using the measurements in table 1 we can compute a plane equation for each side of the rotor in cartesian coordinates:

$$\text{Up plane equation : } z = -9.50 \times 10^{-5}x + 4.83 \times 10^{-4}y + 104.44 \quad (4)$$

$$\text{Down plane equation : } z = -3.69 \times 10^{-5}x + 3.66 \times 10^{-4}y + 104.44 \quad (5)$$

Using eqs. (4) and (5) the gap can be determined, see table 3. The maximum rms of the gap for each sector is 11 μm .

| Measurement point | Sector 1 | | Sector 2 | | Sector 3 | |
|-------------------|----------|------|----------|------|----------|------|
| | Up | Down | Up | Down | Up | Down |
| a | 15 | 3 | 20 | 24 | 15 | 17 |
| b | 14 | 0 | 21 | 24 | 13 | 16 |
| c | 12 | -2 | 20 | 22 | 14 | 22 |
| d | 13 | -3 | 20 | 21 | 17 | 29 |
| e | 0 | -6 | 2 | 0 | 0 | 0 |
| f | 0 | -8 | 3 | 3 | -2 | 1 |
| g | -1 | -10 | 0 | 1 | 0 | 4 |
| h | -2 | -10 | 0 | 0 | -4 | 6 |

Table 3: Gap computed in μm on up and down sides of both sectors of R4-31.

We can then compute the rotor thickness for each point by removing these gaps. If one of the raw values is lower than the corrected thickness we take this lowest value. The value of each point is shown in table 4 at 23°C.

| Measurement point | Sector 1 | Sector 2 | Sector 3 |
|-------------------|----------|----------|----------|
| a | 104.467 | 104.396 | 104.406 |
| b | 104.468 | 104.406 | 104.399 |
| c | 104.463 | 104.417 | 104.390 |
| d | 104.456 | 104.428 | 104.380 |
| e | 104.462 | 104.422 | 104.427 |
| f | 104.460 | 104.428 | 104.420 |
| g | 104.458 | 104.438 | 104.415 |
| h | 104.453 | 104.446 | 104.408 |
| i | 101.652 | 101.648 | 101.649 |
| j | 101.651 | 101.647 | 101.649 |
| k | 101.653 | 101.648 | 101.649 |
| l | 101.653 | 101.648 | 101.648 |

Table 4: Measurements of the thickness in mm for each point at 23°C on L and R sectors of R4-31.

4.2 Radius

Using comparators while the rotor is rotating on its axis we can determine the deformation on both sectors and compute different radii values. Table 5 shows the raw measurements using comparators on L and R sectors. The measurements were made on the up, center and down sides of L and R sectors using three comparators for a total of $5 \times 3 \times 3 = 45$ points (the first and last points are near the edge of the sectors).

| Measurement point | Sector 1 | | | Sector 2 | | | Sector 3 | | |
|-------------------|----------|--------|------|----------|--------|------|----------|--------|------|
| | Up | Center | Down | Up | Center | Down | Up | Center | Down |
| A | 0 | -5 | 5 | 30 | 5 | 0 | 30 | 5 | 0 |
| B | 25 | 15 | 20 | 45 | 20 | 20 | 50 | 25 | 20 |
| C | 25 | 25 | 30 | 50 | 30 | 20 | 60 | 35 | 30 |
| D | 20 | 20 | 25 | 45 | 25 | 20 | 60 | 30 | 20 |
| E | 0 | 0 | 0 | 10 | 0 | 0 | 40 | 10 | 0 |

Table 5: Raw measurements in μm of the comparators for the L and R sectors of R4-31.

The zeroing of the comparators was made arbitrarily close to the edge of the sector. The offsets shown in table 5 are measured relative to this reference.

To compute the radius per measurement point we use the following process: First we compute the mean deformation for one comparator. Then we remove this mean deformation to each measurement of this comparator. The corrected shift value is added to the mean radius of 103.958 mm for sector 1, 103.989 mm for sector 2 and 104.024 mm for sector 3 computed using table 2. This process is repeated for each comparator. The final radius for each point are shown in table 6.

| Measurement point | Sector 1 | | | Sector 2 | | | Sector 3 | | |
|-------------------|----------|---------|---------|----------|---------|---------|----------|---------|---------|
| | Up | Center | Down | Up | Center | Down | Up | Center | Down |
| A | 103.933 | 103.940 | 103.949 | 103.994 | 103.981 | 103.975 | 104.029 | 104.015 | 104.010 |
| B | 103.958 | 103.960 | 103.964 | 104.009 | 103.996 | 103.995 | 104.049 | 104.035 | 104.030 |
| C | 103.958 | 103.970 | 103.974 | 104.014 | 104.006 | 103.995 | 104.059 | 104.045 | 104.030 |
| D | 103.953 | 103.965 | 103.969 | 104.009 | 104.001 | 103.995 | 104.059 | 104.040 | 104.030 |
| E | 103.933 | 103.945 | 103.944 | 103.974 | 103.976 | 103.975 | 104.039 | 104.020 | 104.010 |

Table 6: Radius measurements in mm at 26.9°C for the L and R sectors of R4-31.

5 Characterization of the rotor using a simple model

The geometry used to describe the rotor as a simple model is represented in figure 3.

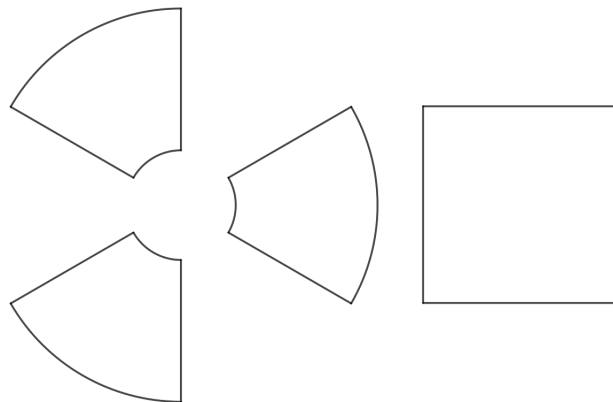


Figure 3: Simple model geometry used to describe the rotor. Left is a front view of the rotor, right is a side view of a sector.

5.1 Thickness

A simple model can use a mean value for the thickness and its uncertainty.

As shown on fig. 2, a total of 16 points were used to compute the thickness of each sector. In this case we will not consider the inner points so that we obtain uniform sectors.

For the simple model we take the thickness as the mean value of table 4: 104.430 mm at 23°C. Since we have a limited number of measurement points, to be conservative we take the thickness uncertainty as the rms of table 4 (27 μm) to which we add linearly the metrology table uncertainty (0.9 μm) and the tool uncertainty (2.0 μm). Therefore, for this simple model, the thickness is 104.430 ± 0.030 mm.

5.2 Radius

For the simple model we take the radius as the mean value of table 6: 103.984 mm at 23°C. Using a linear sum of the rms of table 6 (35.5 μm) and the tool uncertainty (2.0 μm) we take an uncertainty of 38 μm on the mean radius.

We will then consider each sector individually later.

5.3 Analytical model of the rotor

Using the analytical equation of the newtonian force (see eq.1 in [Newtonian calibrator tests during the Virgo O3 data taking](#)) we can compute the strain at 3f.

$F_{i,x}$ is the force of a mass i along the x axis, in the case of three sectors $i = \left[-\frac{2\pi}{3}, 0, \frac{2\pi}{3} \right]$ (with $\epsilon = r/d$):

$$F_{i,x} = \frac{GmM}{d^2} (\cos(\phi) + \epsilon \cos(\theta + \psi) \cos(\phi) - \epsilon''' \sin(\phi) - \epsilon'') [1 + X_i]^{-3/2} \quad (6)$$

We can write the eq.2 of the paper using i and then we have, up to the third order:

$$(1 + X_i)^{-3/2} \approx 1 - \frac{3}{2}X_i + \frac{15}{8}X_i^2 - \frac{35}{16}X_i^3 \quad (7)$$

After computation we are left with the following non null component:

$$F_{i,x} = -\frac{10GmM}{d^2} \epsilon^3 \cos(\phi) \cos^3(\theta + \psi + i) \quad (8)$$

The total force F_x along x is:

$$\begin{aligned} F_x &= \sum_i F_{i,x} = F_{0,x} + F_{\frac{2\pi}{3},x} + F_{-\frac{2\pi}{3},x} \\ &= -\frac{30}{4} \frac{GmM}{d^2} \epsilon^3 \cos(\phi) \cos(3\theta + 3\psi) \end{aligned} \quad (9)$$

Using the following relation of the mass m of the rotor (we will consider the mirror of mass M to be a point with no dimension for this computation):

$$m = \rho_{\text{rot}} \int_{r_{\text{min}}}^{r_{\text{max}}} \int_{-\alpha/2}^{\alpha/2} \int_{-b/2}^{b/2} r dr d\psi db' \quad (10)$$

We have:

$$\begin{aligned} F_x &= -\frac{30}{4} \frac{GM}{d^5} \cos(\phi) \rho_{\text{rot}} b \int_{r_{\text{min}}}^{r_{\text{max}}} r^4 dr \int_{-\alpha/2}^{\alpha/2} \cos(3\theta + 3\psi) d\psi \\ &= -\frac{4}{3} \frac{GM}{d^5} \rho_{\text{rot}} b \cos(\phi) \cos(3\theta) \sin(3\alpha/2) (r_{\text{max}}^5 - r_{\text{min}}^5) \end{aligned} \quad (11)$$

We can now compute the strain at 3f using the following relation:

$$\begin{aligned} \text{strain}(3f_{\text{rot}}) &= \frac{a(3f_{\text{rot}})}{L} = \frac{|F_x|}{ML(2\pi f_{3\text{rot}})^2} \\ &= \frac{G\rho_{\text{rot}} b \sin(3\alpha/2)(r_{\text{max}}^5 - r_{\text{min}}^5)}{4\pi^2 L f_{3\text{rot}}^2 d^5} \cos(\phi) \end{aligned} \quad (12)$$

We compute the analytical strain with the rotor average parameters (using $d = 1.7$ m and an angle $\phi = 34.7^\circ$):

$$\text{strain}(3f) = \frac{1.1625 \times 10^{-19}}{(3f_{\text{rot}})^2} \quad (13)$$

The numerical strain of the mirror at 3f using FROMAGE v1r2 with the rotor average parameters and a punctual mass mirror is:

$$\text{strain}(3f) = \frac{1.1626 \times 10^{-19}}{(3f_{\text{rot}})^2} \quad (14)$$

This value is only 0.009 % larger than the previous value. This small deviation is due to the approximation of the analytical computation since both strains use the same parameters for the rotor and the mirror.

5.4 Effects of the mirror geometry on the 3f signal

Using FROMAGE on this average geometry with a non punctual mass mirror we compute the following 3f strain on the mirror at a distance of 1.7m and an angle of 34.7° :

$$\text{strain}(3f) = \frac{1.1539 \times 10^{-19}}{(3f_{\text{rot}})^2} \quad (15)$$

Comparing the FROMAGE strain (eq. (14)) of a point mass mirror at 3f with the extended mirror (eq. (15)) we obtain a relative deviation of 0.75 %. This may look like a large effect. However a 1 mm change on the radius of the mirror affects the 3f signal by 0.017 % while a 1 mm change on the thickness affects the 3f signal by 0.006 %, the radius and thickness have opposite effects on the 3f signal. This confirms that the NCal signal is weakly dependent on the exact knowledge of the mirror parameters.

5.5 Signal uncertainties for the simple model

The uncertainties considered for this model are displayed in table 7.

| R4-31 rotor parameter simple model (23°C) | | | NCal 3f signal uncertainty | |
|--|---------------------------|-----------------------|--|-----------|
| name | value | uncertainty | formula | value (%) |
| Density ρ (kg.m ⁻³) | 2810.8 | 0.2 | $\delta\rho/\rho$ | 0.007 |
| Thickness b (mm) | 104.430 | 3×10^{-2} | $\delta b/b$ | 0.029 |
| r_{max} (mm) | 103.984 | 3.8×10^{-2} | $5\delta r_{max}/r_{max}$ | 0.180 |
| G (m ³ .kg ⁻¹ .s ⁻²) | 6.67430×10^{-11} | 1.5×10^{-15} | $\delta G/G$ | 0.002 |
| Temperature T (°C) | 23 | 3 | $\frac{\partial h}{\partial T} \frac{\Delta T}{h}$ | 0.021 |
| Quadratic sum | | | | 0.184 |

Table 7: Uncertainties on the amplitude of the calibration signal at 3f from the R4-31 rotor simple model geometry.

6 Characterization of the rotor using an advanced model

6.1 Thickness

A more advanced model can be used considering the deformations on the surfaces of the sectors for better accuracy. Each measurement point of table 4 can be considered as a sub-sector with its own thickness.

The uncertainty on this value is more complex to evaluate. As a conservative approach we use the maximum rms of the deviation to a plane for each sector (10.7 μm see section 4.1) to which we add linearly the uncertainty on the flatness of the measurement table (0.9 μm) as well as the measurement tool (2.0 μm). The total uncertainty on the thickness is 15 μm .

6.2 Radius

On fig. 2 we divided the external sectors in 4 sub-sectors for each sector (blue points). We convert the point of table 6 to the grid of fig. 2 by averaging the two closest values and converting them to 23°C. The results are shown in table 8. We notice that the sector 3 is in average 79 μm larger than the sector 1 and 40 μm larger than the sector 2.

| Radius | Sector 1 | | | Sector 2 | | | Sector 3 | | |
|--------|----------|---------|---------|----------|---------|---------|----------|---------|---------|
| | Up | Center | Down | Up | Center | Down | Up | Center | Down |
| 1 | 103.936 | 103.940 | 103.947 | 103.992 | 103.978 | 103.975 | 104.029 | 104.016 | 104.010 |
| 2 | 103.948 | 103.955 | 103.959 | 104.002 | 103.991 | 103.985 | 104.044 | 104.031 | 104.020 |
| 3 | 103.946 | 103.957 | 103.962 | 104.002 | 103.993 | 103.985 | 104.049 | 104.033 | 104.020 |
| 4 | 103.933 | 103.945 | 103.947 | 103.982 | 103.978 | 103.975 | 104.039 | 104.021 | 104.010 |

Table 8: Radius measurements (in mm at 23°C) for the L and R sectors of R4-31.

The maximum rms of the radii for each sector is 12.9 μm . The tool uncertainty is 2.0 μm . Like for the thickness we use a linear sum and find the uncertainty on both radii to be 15 μm .

6.3 Counterweight

For this rotor, the counterweight used was not machined. The placement of some screws were sufficient to reduce the unbalance of the rotor. This counterweight is made of aluminum 2017 ($\rho_{\text{Al}_{2017}} = 2790 \text{ kg.m}^{-3}$) and the geometry is shown in fig. 4.

The dimensions of the counterweight are an inner radius of 10 mm and an outer radius of 40 mm. The screws and their placement are shown in fig. 4. On hole 1 and 4 are 9.65 mm M3 screws, on hole 2 is a 13.45 mm M3 screw and hole 3 has no screw.

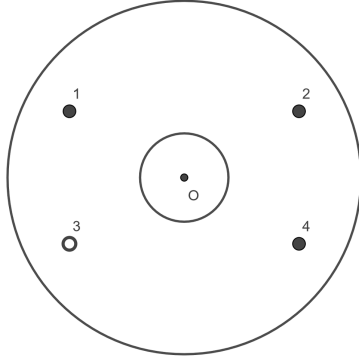


Figure 4: Outline of the counterweight for R4-31.

6.4 Opening angles and asymmetry

The opening angles of the full and empty sectors have been measured using a video microscope with the same method as for R4-01..

6.4.1 Measurements

The measurements are shown in table 9 as offsets from the theoretical value of $\pi/3$. The mean value will be considered as the center value later. A sector labelled n-m corresponds to the empty sector between the full sectors n and m.

| Opening angle | Up offset | Down offset | Mean offset |
|---------------|-----------|-------------|-------------|
| 1 | 0.19 | -3.38 | -1.60 |
| 2 | -0.06 | -1.02 | -0.54 |
| 3 | 0.04 | 3.60 | 1.82 |
| 1-2 | 0.15 | 1.71 | 0.93 |
| 1-3 | -0.16 | 2.36 | 1.10 |
| 2-3 | -0.16 | -3.28 | -1.72 |

Table 9: Offset in mrad of measurements to the theoretical value of the opening angles for the 1,2 and 3 full sectors and 1-2, 1-3 and 2-3 empty sectors of R4-31.

These measurements allow us to compute the signal with different opening angles and an asymmetry between the sectors. These measured opening angles will be included in the advanced model described in the next section.

6.4.2 Uncertainty

The uncertainty on the opening angle α is 0.2 mrad. In the 3f signal computation the angle contributes as $\sin(3\alpha/2)$, the error propagates as $\frac{9}{4}\delta\alpha^2 \sin(3\alpha/2)$ giving an uncertainty of $9 \times 10^{-6} \%$ which is neglectable

6.5 Expected NCal signals and uncertainties

6.5.1 Advanced geometry including chamfers and counterweight

The geometry used to describe the rotor as an advanced model is represented in figure 5. The external parts of the sectors are divided in 3 sub-sectors each to correspond to the different radii determined. In addition we include the counterweight, the screws, the screw holes, the opening angles and asymmetry of the sectors as shown in the FROMAGE layout of fig. 6.

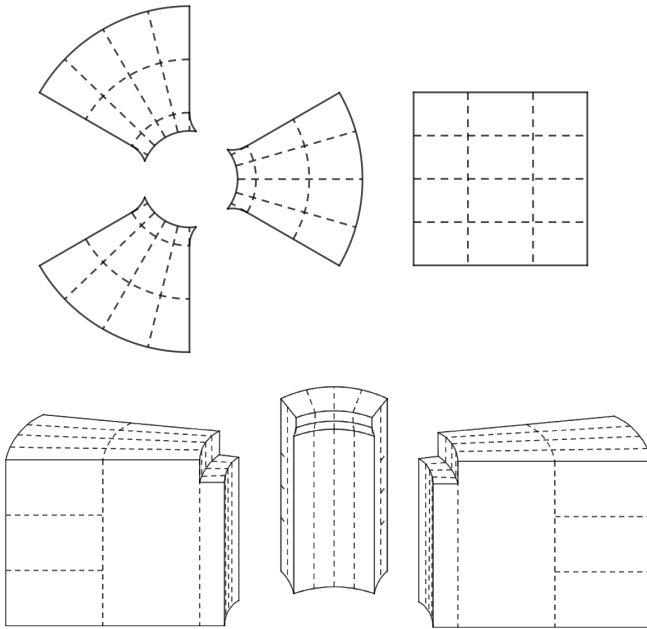


Figure 5: Advanced model geometry used to describe the rotor. Top left is a front view, top right is a side view (external sub-sectors) and bottom is a tilted view of the sectors. Only the 4 external part sectors are divided in 3 sub-sectors each. The chamfers are visible on the inner radius.

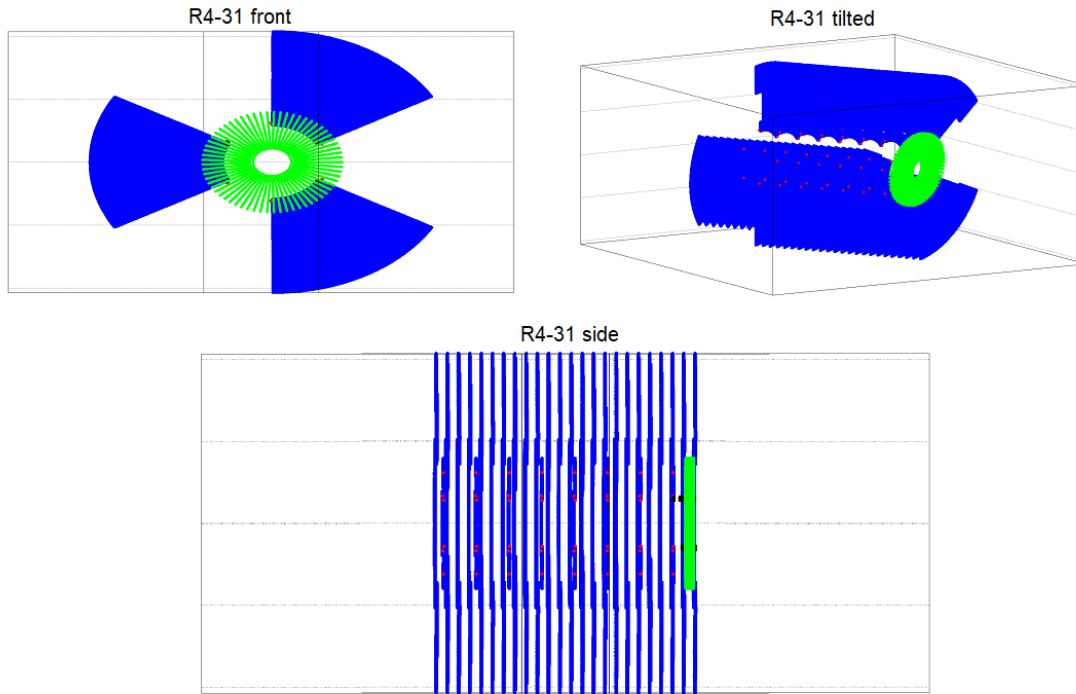


Figure 6: Cloud of points views of the position of each rotor and counterweight element from FROMAGE. Top left is a front view, top right is a general view, bottom is a side view. The rotor sectors are shown in blue, the counterweight in green, the chamfers in red and the screws in black. A grid of 16x65x40 was used for the rotor and the counterweight)

Using FROMAGE on this geometry gives the following strains:

- $\text{strain}(1f) = \frac{9.3529 \times 10^{-20}}{(1f_{rot})^2}$
- $\text{strain}(2f) = \frac{3.6324 \times 10^{-21}}{(2f_{rot})^2}$
- $\text{strain}(3f) = \frac{1.1538 \times 10^{-19}}{(3f_{rot})^2}$

The relative deviation to the simple model at 3f is 0.009%.

6.5.2 Remaining geometry uncertainty

For this rotor we used the same method as R4-01 to reduce the 1f signal. Using 0.38 mm and 0.1 mm positive mass thin blocks on sector 1 and 0.05 mm negative mass and 0.03 mm positive mass thin blocks on sector 3 we managed to reduce the 1f signal by a factor 9.3. The 3f signal is then reduced by $<5 \times 10^{-4}$ %.

In addition we managed to reduce the 2f signal by a factor 9.2 using 0.3 mm and 0.4 mm negative mass thin blocks on sector 3. The 3f signal is also reduced by $<5 \times 10^{-4}$ %.

This value is then taken as the remaining geometry uncertainty.

6.5.3 Uncertainties

To set an uncertainty on the strain(2f) from the description of the geometry we take the difference between the simple model ($\text{strain}(2f) = 1.1539 \times 10^{-19}/(3f)^2$) and the advanced model ($\text{strain}(2f) = 1.1538 \times 10^{-19}/(3f)^2$). This deviation, 0.009%, is reported in table 10 as modelling uncertainty.

The uncertainties considered for this full model are displayed in table 10.

| R4-31 rotor parameter advanced model (23°C) | | | NCal 3f signal uncertainty | |
|--|---------------------------|-----------------------|---|----------------------|
| name | mean value | uncertainty | formula | value (%) |
| Density ρ (kg.m ⁻³) | 2810.8 | 0.2 | $\delta\rho/\rho$ | 0.007 |
| Thickness b sector 1 (12 sub-sectors) (mm) | 104.461 | 1.4×10^{-2} | $\delta b/b$ | 0.013 |
| Thickness b sector 2 (12 sub-sectors) (mm) | 104.422 | | | |
| Thickness b sector 3 (12 sub-sectors) (mm) | 104.406 | | | |
| r_{max} sector 1 (12 ext sub-sectors) (mm) | 103.948 | 1.5×10^{-2} | $5\delta r_{max}/r_{max}$ | 0.071 |
| r_{max} sector 2 (12 ext sub-sectors) (mm) | 103.987 | | | |
| r_{max} sector 3 (12 ext sub-sectors) (mm) | 104.027 | | | |
| G (m ³ .kg ⁻¹ .s ⁻²) | 6.67430×10^{-11} | 1.5×10^{-15} | $\delta G/G$ | 0.002 |
| Temperature T (°C) | 23 | 3 | $\left \frac{\partial h}{\partial T} \right \frac{\Delta T}{h}$ | 0.021 |
| Modelling Uncertainty | | | | 0.009 |
| FROMAGE grid uncertainty | | | | 0.005 |
| Opening angle and sector asymmetry uncertainty | | | | $< 5 \times 10^{-4}$ |
| Remaining geometry uncertainty | | | | $< 5 \times 10^{-4}$ |
| Total uncertainty from the rotor (quadratic sum) | | | | 0.077 |

Table 10: Uncertainties on the amplitude of the calibration signal at 3f from the R4-31 rotor advanced model geometry at 23°C.

A Appendix

```
### This is a cfg file for a more realistic geometry of the mirror and the Virgo NCal R4-31 (2022)
```

```
### ALL THE OBJECTS ARE DEFINED IN THE MIRROR'S FRAME (0,x,y,z),
### with 0 the center of the mirror, x axis along the ITF's beam toward the beam-splitter,
### y axis orthogonal to x in the plane of the ITF,
### z axis orthogonal to the plane of the ITF upward
```

```
### MIRROR DEFINITION
```

```
GRID_SIZE 12 30 8
```

```
CYLINDER 2202. 0 0.175 0.2 360 0 0 0
```

```
GRID_SIZE 1 1 1
```

```
# Defining the flats on the edge of the mirror
```

```
CUT_CYL 2202. 0.175 0.2 0.05 0 0
```

```
CUT_CYL 2202. 0.175 0.2 0.05 0 180
```

```
# Defining the ears and anchors of the mirror
```

```
CUBOID 2202. 0.090 0.010 0.015 0 0.1782 -0.0125
```

```
CUBOID 2202. 0.090 0.010 0.015 0 -0.1782 -0.0125
```

```
CUBOID 2202. 0.039 0.008 0.008 -0.02 -0.1772 -0.024
```

```
CUBOID 2202. 0.039 0.008 0.008 -0.02 0.1772 -0.024
```

```
CUBOID 2202. 0.039 0.008 0.008 0.02 -0.1772 -0.024
```

```
CUBOID 2202. 0.039 0.008 0.008 0.02 0.1772 -0.024
```

```
### ROTOR DEFINITION: CYLINDER DENSITY INNER_RADIUS OUTER_RADIUS THICKNESS OPEN_ANGLE r z theta
```

```
ROTOR_CYLINDRICAL 1.7 34.7 0 0
```

```
### COUNTERWEIGHT 2790.
```

```
GRID_SIZE 16 65 40
```

```
CYLINDER 2790. 0.010 0.040 0.003 360 0 0.048020 0
```

```
### SCREW HOLES
```

```
GRID_SIZE 4 4 4
```

```
CYLINDER -2810.8 0 0.001625 0.012 360 0.03 0.04482638004946 150
```

```
CYLINDER -2810.8 0 0.001625 0.012 360 0.03 0.04482388005536 30
```

```
CYLINDER -2810.8 0 0.001625 0.012 360 0.03 0.04482638004946 210
```

```
CYLINDER -2810.8 0 0.001625 0.012 360 0.03 0.04482388005536 330
```

```
### SCREWS COUNTERWEIGHT
```

```
CYLINDER -4810. 0 0.001625 0.003 360 0.03 0.0480195710931835 150
```

```
CYLINDER 7600. 0 0.001625 0.00665 360 0.03 0.04750138004946 150
```

```
CYLINDER -4810. 0 0.001625 0.003 360 0.03 0.0480195710931835 30
```

```
CYLINDER 7600. 0 0.001625 0.01045 360 0.03 0.04560138004946 30
```

```
CYLINDER -4910. 0 0.001625 0.003 360 0.03 0.0480195710931835 330
```

```
CYLINDER 7600. 0 0.001625 0.00665 360 0.03 0.04750138004946 330
```

```
# TRES RAPIDE
```

```
#GRID_SIZE 4 4 4
```

```
# RAPIDE
GRID_SIZE 8 17 14
# LENT
#GRID_SIZE 8 65 40

### Sector 1

## Inner part
OUTER_FILLET 2810.8 0.029 0.101652 -0.002807 0.01 -7.4886 157.5343
CYLINDER 2810.8 0.029 0.04 0.101652 14.9772 0 -0.002807 157.5343
CYLINDER 2810.8 0.029 0.04 0.101651 14.9772 0 -0.002808 172.5114
CYLINDER 2810.8 0.029 0.04 0.101653 14.9772 0 -0.002807 187.4886
CYLINDER 2810.8 0.029 0.04 0.101653 14.9772 0 -0.002807 202.4657
OUTER_FILLET 2810.8 0.029 0.101653 -0.002807 0.01 7.4886 202.4657

## Middle part
CYLINDER 2810.8 0.04 0.072 0.104462 14.9772 0 0 157.5343
CYLINDER 2810.8 0.04 0.072 0.104460 14.9772 0 0 172.5114
CYLINDER 2810.8 0.04 0.072 0.104458 14.9772 0 0 187.4886
CYLINDER 2810.8 0.04 0.072 0.104453 14.9772 0 0 202.4657

## Outer part
CYLINDER 2810.8 0.072 0.103936 0.0348222511526267 15.0028 0 0.0348222511526267 157.4958
CYLINDER 2810.8 0.072 0.103940 0.0348222511526267 14.9772 0 0 157.5343
CYLINDER 2810.8 0.072 0.103947 0.0348222511526267 14.9515 0 -0.0348222511526267 157.5727

CYLINDER 2810.8 0.072 0.103948 0.0348225739591634 15.0028 0 0.0348225739591634 172.4986
CYLINDER 2810.8 0.072 0.103955 0.0348225739591634 14.9772 0 0 172.5114
CYLINDER 2810.8 0.072 0.103959 0.0348225739591634 14.9515 0 -0.0348225739591634 172.5242

CYLINDER 2810.8 0.072 0.103946 0.0348211240236447 15.0028 0 0.0348211240236447 187.5014
CYLINDER 2810.8 0.072 0.103957 0.0348211240236447 14.9772 0 0 187.4886
CYLINDER 2810.8 0.072 0.103962 0.0348211240236447 14.9515 0 -0.0348211240236447 187.4786

CYLINDER 2810.8 0.072 0.103933 0.0348186765700527 15.0028 0 0.0348186765700527 202.5042
CYLINDER 2810.8 0.072 0.103945 0.0348186765700527 14.9772 0 0 202.4657
CYLINDER 2810.8 0.072 0.103947 0.0348186765700527 14.9515 0 -0.0348186765700527 202.4273

### Sector 2

## Inner part
OUTER_FILLET 2810.8 0.029 0.101648 -0.002785 0.01 -7.4961 37.5196
CYLINDER 2810.8 0.029 0.04 0.101648 14.9923 0 -0.002785 37.5196
CYLINDER 2810.8 0.029 0.04 0.101647 14.9923 0 -0.002786 52.5119
CYLINDER 2810.8 0.029 0.04 0.101648 14.9923 0 -0.002785 67.5041
CYLINDER 2810.8 0.029 0.04 0.101648 14.9923 0 -0.002785 82.4964
OUTER_FILLET 2810.8 0.029 0.101648 -0.002785 0.01 7.4961 82.4964

## Middle part
CYLINDER 2810.8 0.04 0.072 0.104422 14.9923 0 0 37.5196
CYLINDER 2810.8 0.04 0.072 0.104428 14.9923 0 0 52.5119
CYLINDER 2810.8 0.04 0.072 0.104438 14.9923 0 0 67.5041
CYLINDER 2810.8 0.04 0.072 0.104446 14.9923 0 0 82.4964

## Outer part
CYLINDER 2810.8 0.072 0.103992 0.0347985845418133 14.9991 0 0.0347985845418133 37.5093
```

```
CYLINDER 2810.8 0.072 0.103978 0.0347985845418133 14.9923 0 0 37.5196
CYLINDER 2810.8 0.072 0.103975 0.0347985845418133 14.9854 0 -0.0347985845418133 37.5299

CYLINDER 2810.8 0.072 0.104002 0.03480191786728 14.9991 0 0.03480191786728 52.5084
CYLINDER 2810.8 0.072 0.103991 0.03480191786728 14.9923 0 0 52.5119
CYLINDER 2810.8 0.072 0.103985 0.03480191786728 14.9854 0 -0.03480191786728 52.5153

CYLINDER 2810.8 0.072 0.104002 0.0348055845252933 14.9991 0 0.0348055845252933 67.5075
CYLINDER 2810.8 0.072 0.103993 0.0348055845252933 14.9923 0 0 67.5041
CYLINDER 2810.8 0.072 0.103985 0.0348055845252933 14.9854 0 -0.0348055845252933 67.5007

CYLINDER 2810.8 0.072 0.103982 0.0348092511833067 14.9991 0 0.0348092511833067 82.5066
CYLINDER 2810.8 0.072 0.103978 0.0348092511833067 14.9923 0 0 82.4964
CYLINDER 2810.8 0.072 0.103975 0.0348092511833067 14.9854 0 -0.0348092511833067 82.4861

### Sector 3

## Inner part
OUTER_FILLET 2810.8 0.029 0.101649 -0.002769 0.01 -7.5130 277.5308
CYLINDER 2810.8 0.029 0.04 0.101649 15.0261 0 -0.002769 277.5308
CYLINDER 2810.8 0.029 0.04 0.101649 15.0261 0 -0.002769 292.5569
CYLINDER 2810.8 0.029 0.04 0.101649 15.0261 0 -0.002769 307.5830
CYLINDER 2810.8 0.029 0.04 0.101648 15.0261 0 -0.002769 322.6090
OUTER_FILLET 2810.8 0.029 0.101648 -0.002769 0.01 7.5130 322.6090

## Middle part
CYLINDER 2810.8 0.04 0.072 0.104427 15.0261 0 0 277.5308
CYLINDER 2810.8 0.04 0.072 0.104420 15.0261 0 0 292.5569
CYLINDER 2810.8 0.04 0.072 0.104415 15.0261 0 0 307.5830
CYLINDER 2810.8 0.04 0.072 0.104408 15.0261 0 0 322.6090

## Outer part
CYLINDER 2810.8 0.072 0.104029 0.03480191786728 15.0006 0 0.03480191786728 277.5691
CYLINDER 2810.8 0.072 0.104016 0.03480191786728 15.0261 0 0 277.5308
CYLINDER 2810.8 0.072 0.104010 0.03480191786728 15.0516 0 -0.03480191786728 277.4925

CYLINDER 2810.8 0.072 0.104044 0.0347995845394533 15.0006 0 0.0347995845394533 292.5697
CYLINDER 2810.8 0.072 0.104031 0.0347995845394533 15.0261 0 0 292.5569
CYLINDER 2810.8 0.072 0.104020 0.0347995845394533 15.0516 0 -0.0347995845394533 292.5441

CYLINDER 2810.8 0.072 0.104049 0.0347965845465333 15.0006 0 0.0347965845465333 307.5702
CYLINDER 2810.8 0.072 0.104033 0.0347965845465333 15.0261 0 0 307.5830
CYLINDER 2810.8 0.072 0.104020 0.0347965845465333 15.0516 0 -0.0347965845465333 307.5957

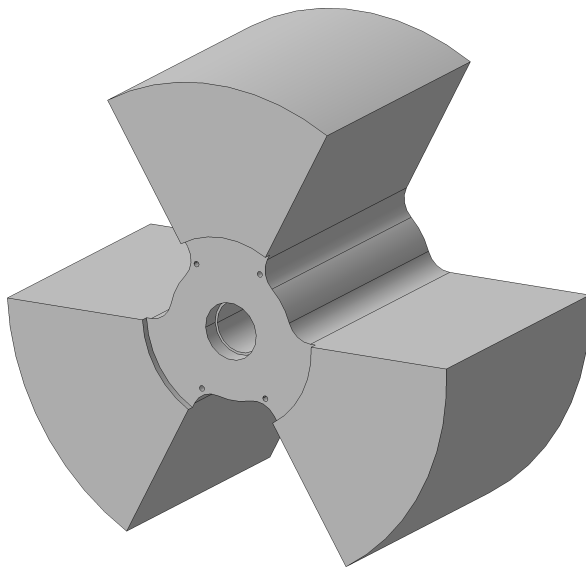
CYLINDER 2810.8 0.072 0.104039 0.0347932512210667 15.0006 0 0.0347932512210667 322.5708
CYLINDER 2810.8 0.072 0.104021 0.0347932512210667 15.0261 0 0 322.6090
CYLINDER 2810.8 0.072 0.104010 0.0347932512210667 15.0516 0 -0.0347932512210667 322.6473
```

GENERAL PARAMETERS

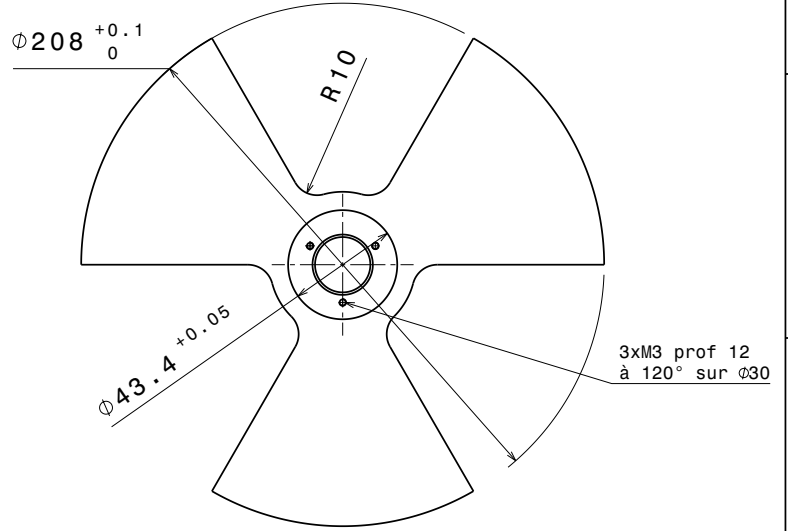
STEP 22.5 16

ARM_LENGTH 3000

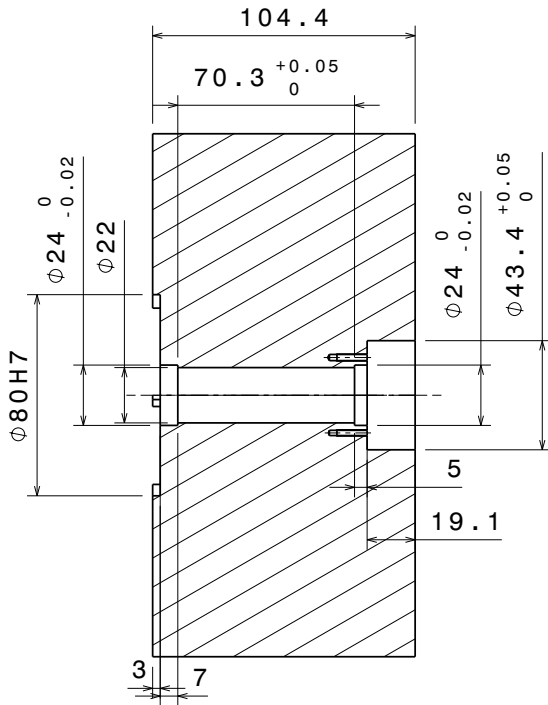
SIGNAL 3



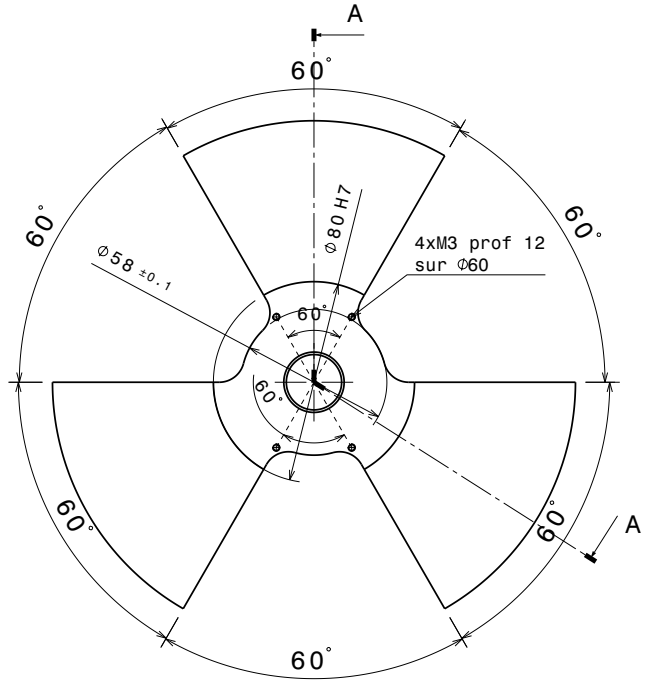
Vue isométrique
Echelle : 1:2




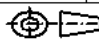
Vue de derrière
Echelle : 1:2



Coupe A-A
Echelle : 1:2



Vue de face
Echelle : 1:2

| | | | | | |
|---|-----|----------------|-----------------------|---|-------------------|
| N° | 3 | AW7075 | Traitement de surface | 5 Kg | Dessin d'ensemble |
| Rug. gén. : Ra = 3,2 | Qté | Matière | Chanfreins: 0,2 à 45° | Masse | VIRGO Ncal |
| CNRS - IN2P3 | | ROTOR 3 bras_S | | | |
|  | | Dessiné par : | Vérifié par : | A3 | Numéro |
| 23, rue du Loess - BP 28 67037 Strasbourg Cedex 02 | | Valeria ZETER | le 12/04/2022 |  | Echelle 1:2 |
| | | | | Révision | |

Copyright IN2P3 / IRIS